
The Soluble Proteome of the *Drosophila* Antenna

Robert R.H. Anholt¹ and Taufika Islam Williams²

¹Departments of Biology and Genetics and W. M. Keck Center for Behavioral Biology, Box 7617, North Carolina State University, Raleigh, NC 27695-7617, USA and ²Department of Chemistry, Box 8204, North Carolina State University, Raleigh, NC 27695-8204, USA

Correspondence to be sent to: Robert R.H. Anholt, Department of Biology, Box 7617, North Carolina State University, Raleigh, NC 27695-7617, USA. e-mail: anholt@ncsu.edu

Accepted September 21, 2009

Abstract

The olfactory system of *Drosophila melanogaster* is one of the best characterized chemosensory systems. Identification of proteins contained in the third antennal segment, the main olfactory organ, has previously relied primarily on immunohistochemistry, and although such studies and in situ hybridization studies are informative, they focus generally on one or few gene products at a time, and quantification is difficult. In addition, purification of native proteins from the antenna is challenging because it is small and encased in a hard cuticle. Here, we describe a simple method for the large-scale detection of soluble proteins from the *Drosophila* antenna by chromatographic separation of tryptic peptides followed by tandem mass spectrometry with femtomole detection sensitivities. Examination of the identities of these proteins indicates that they originate both from the extracellular perilymph and from the cytoplasm of disrupted cells. We identified enzymes involved with intermediary metabolism, proteins associated with regulation of gene expression, nucleic acid metabolism and protein metabolism, proteins associated with microtubular transport, 8 odorant-binding proteins, protective enzymes associated with antibacterial defense and defense against oxidative damage, cuticular proteins, and proteins of unknown function, which represented about one-third of all soluble proteins. The procedure described here opens the way for precise quantification of any target protein in the *Drosophila* antenna and should be readily applicable to antennae from other insects.

Key words: chemosensation, mass spectrometry, odorant-binding proteins, olfaction, proteomics

Introduction

The olfactory system of *Drosophila melanogaster* has emerged as one of the best characterized chemosensory systems. Odorants are recognized by sensory neurons housed in sensilla of the third antennal segment and the maxillary palps, the main olfactory organs, as well as chemosensory neurons on the tarsi, wing margins, and female reproductive organs. Olfactory sensory neurons in basiconic sensilla of the antenna and maxillary palps express odorant receptors that contain 7 transmembrane domains (Clyne et al. 1999; Gao and Chess 1999; Vosshall et al. 1999), but differ from classical G protein-coupled receptors in membrane orientation (Benton et al. 2006) and transduction mechanism, as odorant activation results in the opening of a cation channel formed by a complex between a unique olfactory receptor and the universal Or83b receptor (Sato et al. 2008; Wicher et al. 2008). The molecular receptive fields and activation properties of a large fraction of odorant receptors have been characterized by elegant electrophysiological studies (de Bruyne et al. 1999, 2001; Hallem et al. 2004; Hallem and Carlson

2006), and projections of cells expressing defined receptors have been mapped to individual glomeruli in the antennal lobes (Vosshall et al. 2000). Olfactory sensory neurons in coeloconic sensilla express yet another family of odorant receptors that resemble ionotropic glutamate receptors with distinct ligand specificities, including responses to amines (Benton et al. 2009). In addition to odorant receptors, a large family of odorant-binding proteins (Obps) that are secreted by supporting cells into the antennal perilymph has been characterized (Galindo and Smith 2001; Hekmat-Scafe et al. 2002), and members of this family have been implicated in pheromone detection (Xu et al. 2005; Laughlin et al. 2008), host plant selection (Matsuo et al. 2007), and combinatorial recognition of general odorants (Wang et al. 2007).

Transcriptional profiling studies have shown that expression of the chemosensory repertoire of *Drosophila* is dynamic and changes under different developmental, environmental, and physiological conditions (Zhou et al. 2009). Clearly, it would be of value to correlate overall protein levels with

changes in transcript abundance. Previously, the expression of Obps and odorant receptors, as well as proteins implicated in removal of xenobiotics, including odorants, has been characterized by in situ hybridization (McKenna et al. 1994; Pikielny et al. 1994; Clyne et al. 1999; Vosshall et al. 1999; Rollmann et al. 2005), immunohistochemistry (Hekmat-Scafe et al. 1997), enhancer trap (Riesgo-Escovar et al. 1992; Anholt et al. 1996), and transgenic drivers using the GAL4-UAS binary expression system (Vosshall et al. 2000; Galindo and Smith 2001). Although such studies have been highly informative, they focus generally on one or few gene products at a time and quantification by any of these methods is difficult. Furthermore, biochemical purification of native proteins from the antenna is challenging due to the small size of the *Drosophila* antenna and because olfactory sensory neurons are encased in a hard cuticle.

Here, we describe a simple method for the large-scale detection of soluble proteins from the *Drosophila* antenna using chromatographic separation of tryptic peptides by nano-LC followed by tandem mass spectrometry (MS/MS), with femtomole detection sensitivities. Confident protein identifications are obtained when LC retention time data are combined with accurate mass measurements and MS/MS fingerprints. The procedure described here opens the way for precise quantification of any target protein in the *Drosophila* antenna and should be readily applicable to antennae from other insects, including disease vectors, such as mosquitoes and urban pests, such as cockroaches, which rely on olfactory input for host identification, mating, and oviposition site selection.

Materials and methods

Drosophila stocks and sample preparation

Isogenic *D. melanogaster* of the *Canton S* (*B*) strain were reared on standard cornmeal molasses agar medium at 25 °C and 70% humidity under a 12 h light:dark cycle. Antennae were dissected by hand under a stereomicroscope and immediately placed in microcentrifuge tubes on dry ice. Duplicate pools of 120 antennae from males and females were obtained separately. The antennae were subjected to osmotic lysis by 2 freeze-thaw cycles in 50- μ L distilled water followed by homogenization with a small pestle and centrifugation to remove nonsoluble material. The supernatants were recovered, and 32- μ L samples were evaporated to dryness and reconstituted in 25.5 μ L of 50 mM NH_4HCO_3 without introduction of detergents. For tryptic digestion of proteins, 1.5 μ L of 100 mM aqueous dithiothreitol was added to each sample, and the samples were heated at 95 °C for 5 min. Upon cooling to room temperature, 3 μ L of 100 mM aqueous iodoacetamide was added, and the resulting solution incubated at room temperature in the dark for 20 min. This was preceded by the addition of trypsin (1 μ L of a 0.1 $\mu\text{g}/\mu\text{L}$ trypsin solution in 1 mM HCl). Digestion was carried out at 37 °C for 3 h, following which another

1 μ L of trypsin solution was added and samples were incubated at 30 °C overnight. Trypsin was quenched by addition of 1.5 μ L of 5% formic acid. Samples were then evaporated to dryness, reconstituted in 100 μ L of LC mobile phase A (98% H_2O , 2% acetonitrile, and 0.2% formic acid), and filtered with 10 kDa molecular weight cut off filters (Millipore number 42407) prior to LC/MS/MS analyses. Serial dilutions of the sample solutions up to 1000-fold were performed prior to analysis to determine the optimum concentration for sample introduction into the instrument.

Mass spectrometry

Reversed phase high-performance liquid chromatography separation and MS detection were performed using an Eksigent nano-LC-2D system with an autosampler coupled to a hybrid LTQ-FT Ultra mass spectrometer from Thermo Scientific, Inc. The nano-LC was operated with a “continuous vented column” configuration for in-line trap and elute (Andrews et al. 2009). The analytical column was a self-packed 75- μm inner diameter (i.d.) fused silica PicoFrit capillary with 15 cm of Magic C18AQ stationary phase. The trap and dummy columns were self-packed 75 μm i.d. fused silica IntegraFrit capillaries with 5 cm and 20 cm of Magic C18AQ stationary phase, respectively. LC solvents used are mobile phase A and mobile phase B (acetonitrile/ $\text{H}_2\text{O}/\text{H}$ formic acid [98/2/0.2% by volume]). Blank runs were performed after every sample run. Sample injections ranged from 2 to 5 μL on column. Analytical separations were run on the nanoflow pump at 500 nL/min, initially maintaining a composition of 2% B. The MS method consisted of 4 events: a precursor scan followed by 3 data-dependent tandem MS scans of the first, second, and third most abundant peaks in the ion trap. A high resolving power precursor scan of the eluted peptides was obtained using the LTQ-FT with the 3 most abundant ions selected for MS/MS in the ion trap through dynamic exclusion. The instrument was externally calibrated according to the manufacturer’s protocol.

Data analysis

The nano-LC/MS/MS data files were processed by Sequest (Bioworks, ThermoFisher Scientific, Inc.; Eng et al. 1994) and Mascot (Matrix Science; Perkins et al. 1999) for protein identifications. These algorithms apply similar general approaches in assigning peptides detected in MS/MS spectra to those in a sequence database. However, the principles behind their mathematical operations are significantly different. Mascot applies a probabilistic metric to determine the likelihood that a fragmented peptide produced an observed MS/MS spectrum. Sequest, on the other hand, applies empirical and correlation measurements to score the alignment between observed and predicted spectra, among other important differences. Batch searching of LC/MS/MS data was performed using the *D. melanogaster* protein database from InterPro (www.ebi.ac.uk/interpro).

Results and discussion

Combining the high mass measurement accuracies of the LTQ-FT mass analyzer with tandem MS fragmentation data and nano-LC retention times allows for confident protein identifications with minimal sample consumption. A representative nano-LC/MS/MS identification of an Obp (PBP2_DROME Pheromone-binding protein-related protein 2 precursor) released from a female antenna is presented in Figure 1. Tandem mass spectrometric analysis of eluted chromatographic peaks allowed for the identification of approximately 100 proteins through Sequest and Mascot database search algorithms. Sequest was able to identify 30 proteins (Table 1), whereas analysis with Mascot resulted in

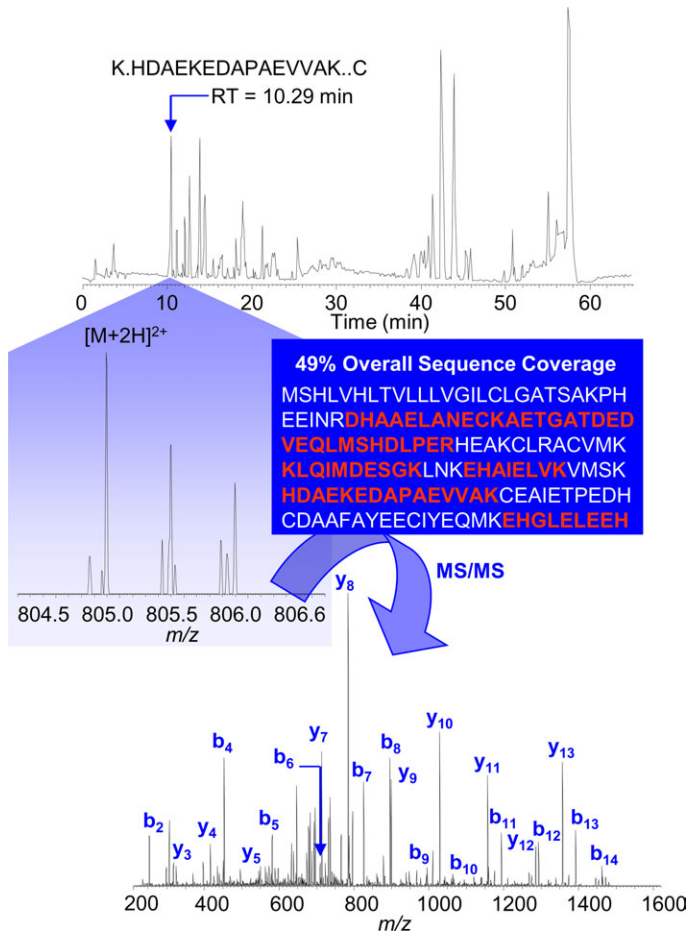


Figure 1 nano-LC/MS/MS identification of PBP2_DROME Pheromone-binding protein-related protein 2 precursor—*Drosophila melanogaster*. A tryptic peptide, which eluted from the nano-LC column at a retention time (RT) of 10.29 min (chromatogram shown at the top of the figure), is identified by nano-LC/MS/MS (with database searching) to be derived from PBPRP2 precursor protein. The MS spectrum for this peptide is shown in the center of the figure. The ionized, doubly charged peptide is subjected to dynamic exclusion and fragmentation to generate an MS/MS fingerprint (lower spectrum) that conclusively verifies its molecular structure. As many as 11 peptides derived from PBPRP2 precursor protein were detected in total, providing 49% sequence coverage (shown in red font in the middle of the figure).

Table 1 Soluble protein identifications (30 total) for *Drosophila melanogaster* antennae by Sequest (Obps are highlighted in bold font)

Protein identification	<i>P</i>	Score (XC)
ATPB_DROME ATP synthase subunit beta, mitochondrial precursor	1.6×10^{-13}	5.42×10^1
PBP2_DROME pheromone-binding protein-related protein 2 precursor	2.5×10^{-12}	1.28×10^2
Q7K084_DROME RH04549p	3.8×10^{-8}	6.02×10^1
SODC_DROME superoxide dismutase [Cu-Zn]	7.5×10^{-8}	5.02×10^1
Q8SY92_DROME RH21971p	8.6×10^{-8}	4.02×10^1
O16157_DROME calcium-binding protein	2.0×10^{-7}	3.02×10^1
Q9VEB1_DROME CG7998-PA	3.0×10^{-7}	3.62×10^1
PRDX1_DROME peroxiredoxin 1	3.3×10^{-7}	1.42×10^1
BNB_DROME protein bangles and beads	5.1×10^{-7}	5.03×10^1
ATPA_DROME ATP synthase subunit alpha, mitochondrial precursor	5.1×10^{-7}	6.22×10^1
OBP56D_DROME general Obp 56d precursor	7.7×10^{-7}	2.02×10^1
G3P1_DROME glyceraldehyde-3-phosphate dehydrogenase	8.5×10^{-7}	5.62×10^1
PBP6_DROME pheromone-binding protein-related protein 6 precursor	1.8×10^{-6}	6.02×10^1
Q7KUB0_DROME CG7176-PA, isoform A	2.2×10^{-6}	6.01×10^1
ENO_DROME isoform 1 of P15007	3.4×10^{-6}	4.22×10^1
Q9VQF7_DROME CG9894-PA, isoform A	6.1×10^{-6}	2.02×10^1
Q9VTC3_DROME CG6409-PA	9.5×10^{-6}	4.02×10^1
P91941_DROME CG10297-PA	2.9×10^{-5}	2.42×10^1
O16043_DROME CG2207-PA, isoform A	3.0×10^{-5}	2.02×10^1
PBP5_DROME pheromone-binding protein-related protein 5 precursor	4.8×10^{-5}	2.81×10^1
OB10_DROME putative Obp A10 precursor	4.9×10^{-5}	4.02×10^1
GSTT1_DROME glutathione S-transferase 1-1	6.1×10^{-5}	2.22×10^1
ALF_DROME isoform Gamma of P07764	8.7×10^{-5}	4.22×10^1
EST6_DROME esterase-6 precursor	1.0×10^{-4}	6.02×10^1
APLP_DROME apolipoporphins precursor	1.1×10^{-4}	7.82×10^1
PBP3_DROME pheromone-binding protein-related protein 3 precursor	1.1×10^{-4}	6.62×10^1
NPLP2_DROME neuropeptide-like 2 precursor	1.4×10^{-4}	2.02×10^1
ACT1_DROME actin-5C	3.4×10^{-4}	3.41×10^1
Q8SXA6_DROME GH20168p	5.5×10^{-4}	2.62×10^1
CISY_DROME isoform A of Q9W401	1.9×10^{-3}	6.01×10^1

XC is the correlation score.

Table 2 Soluble protein identifications (94 total) for *Drosophila melanogaster* antennae by Mascot (Obps are highlighted in bold font; protein mass is in Daltons)

Accession numbers	Protein identification	Protein score	Protein mass	Protein matches
sp O02649 CH60_DROME	60 kDa heat shock protein, mitochondrial	35	60 885	1
sp P07487 G3P2_DROME	Glyceraldehyde-3-phosphate dehydrogenase 2	212	35 518	6
sp P08171 EST6_DROME	Esterase-6	168	61 486	4
sp P15007-1 ENO_DROME	Isoform B of enolase	163	54 561	4
sp P18106-3 FPS_DROME	Isoform C of tyrosine-protein kinase Fps85D	23	54 963	1
sp P20432 GSTT1_DROME	Glutathione S-transferase 1-1	120	24 022	3
sp P29746 BNB_DROME	Protein bangles and beads	305	45 902	6
sp P31409 VATB_DROME	V-type proton ATPase subunit B	34	54 800	1
sp P34739 TTF2_DROME	Transcription termination factor 2	37	118 759	2
sp P35381 ATPA_DROME	ATP synthase subunit alpha, mitochondrial	183	59 612	4
sp P41073-1 PEP_DROME	Isoform B of zinc finger protein on ecdysone puffs	22	78 570	1
sp P46863 KL61_DROME	Bipolar kinesin KRP-130	26	121 772	1
sp P51123-1 TAF1_DROME	Isoform B of transcription initiation factor TFIID subunit 1	25	240 307	1
sp P54192 PBP2_DROME	Pheromone-binding protein-related protein 2	509	17 170	11
sp P54193 PBP3_DROME	Pheromone-binding protein-related protein 3	80	17 657	4
sp P54195 PBP5_DROME	Pheromone-binding protein-related protein 5	39	15 484	1
sp P55830 RS3A_DROME	40S ribosomal protein S3a	31	30 565	1
sp P61851 SODC_DROME	Superoxide dismutase [Cu-Zn]	333	15 974	6
sp P62152 CALM_DROME	Calmodulin	38	16 800	2
sp Q05825 ATPB_DROME	ATP synthase subunit beta, mitochondrial	186	54 074	5
sp Q09101-1 HIG_DROME	Isoform 3 of locomotion-related protein hikaru genki	26	108 557	1
sp Q23970 PBP6_DROME	Pheromone-binding protein-related protein 6	137	16 500	6
sp Q24120 CAPU_DROME	Protein cappuccino	23	114 705	1
sp Q24407 ATP5J_DROME	ATP synthase-coupling factor 6, mitochondrial	68	11 928	1
sp Q27377 OB10_DROME	Putative Obp A10	130	18 111	2
sp Q32KD2 SETB1_DROME	Histone-lysine N-methyltransferase eggless	38	143 852	1
sp Q8SY61 OB56D_DROME	General Obp 56d	181	14 452	4
sp Q9NJG9-1 SUZ12_DROME	Isoform 1 of polycomb protein Su(z)12	34	101 011	1
sp Q9V3P0 PRDX1_DROME	Peroxioredoxin 1	118	21 952	3
sp Q9V785 3BP5H_DROME	SH3 domain-binding protein 5 homolog	22	54 060	1
sp Q9V7N5-1 VATC_DROME	Isoform D of V-type proton ATPase subunit C	26	79 776	1
sp Q9VPS5 CH60B_DROME	60 kDa heat shock protein homolog 1, mitochondrial	34	68 992	1
sp Q9VU58 NPLP2_DROME	Neuropeptide-like 2	92	9463	1
sp Q9W1C9 PEB3_DROME	Ejaculatory bulb-specific protein 3	73	14 759	1
sp Q9W1R5 VIR_DROME	Protein virilizer	29	210 751	1
sp Q9W401-1 CISY_DROME	Isoform A of probable citrate synthase, mitochondrial	34	51 713	3
tr A1Z6K9 A1Z6K9_DROME	CG17994-PA	25	59 821	1
tr A1Z7Z9 A1Z7Z9_DROME	CG1625-PA	26	129 850	2

Table 2 Continued

Accession numbers	Protein identification	Protein score	Protein mass	Protein matches
tr A1ZA97 A1ZA97_DROME	CG8424-PA	80	62456	2
tr A4V3F9 A4V3F9_DROME	Fructose-bisphosphate aldolase	193	39 251	5
tr A8DZ12 A8DZ12_DROME	CG15140-PA (Fragment)	21	30 108	4
tr A8JV09 A8JV09_DROME	CG4532-PF, isoform F	21	140 127	1
tr A8QI20 A8QI20_DROME	CG41561-PA (Fragment)	31	40 471	1
tr O16043 O16043_DROME	CG2207-PA, isoform A (CG2207-PB, isoform B) (CG2207-PF, isoform F) (LD21289p) (Anon1A4)	90	18 812	1
tr O97102 O97102_DROME	CG4494-PA	82	10 175	1
tr Q0E8L0 Q0E8L0_DROME	CG8486-PC, isoform C	26	305 750	1
tr Q4ABG9 Q4ABG9_DROME	CG33715-PE, isoform E	22	1 064 061	2
tr Q4V5I6 Q4V5I6_DROME	IP07112p (IP06812p) (CG14810-PA)	26	22 874	1
tr Q59DY8 Q59DY8_DROME	CG33552-PA	24	18 848	1
tr Q7JND6 Q7JND6_DROME	Cuticle protein ACP65A	123	10 773	1
tr Q7K084 Q7K084_DROME	RH04549p (CG2297-PA) Obp 44a	213	16 135	5
tr Q7K088 Q7K088_DROME	RH03850p (CG8462-PA) Obp 56e	44	14 505	1
tr Q7K2B0 Q7K2B0_DROME	LD11455p (CG7137-PA)	26	40 605	1
tr Q7KMR7 Q7KMR7_DROME	Thioredoxin-like protein TXL	25	32 140	1
tr Q7KTB7 Q7KTB7_DROME	CG6214-PM, isoform M	26	174 219	1
tr Q7KUB0 Q7KUB0_DROME	CG7176-PA, isoform A (CG7176-PE, isoform E) (CG7176-PF, isoform F)	192	47 030	6
tr Q8I940 Q8I940_DROME	CG1271-PD, isoform D	22	60 539	1
tr Q8IRD3 Q8IRD3_DROME	Glutathione peroxidase	23	26 620	1
tr Q8MLS0 Q8MLS0_DROME	CG13551-PC, isoform C	65	9711	1
tr Q8MSI2 Q8MSI2_DROME	GH15296p (CG15848-PA)	172	21 919	4
tr Q8MSU4 Q8MSU4_DROME	CG2097-PA	26	133 020	2
tr Q8MYW5 Q8MYW5_DROME	CG14667-PA, isoform A	20	30 574	1
tr Q8SWW8 Q8SWW8_DROME	LD18186p (CG12489-PA)	25	74 562	1
tr Q8SX06 Q8SX06_DROME	RH33338p (CG14141-PA)	30	18 788	1
tr Q8SXZ0 Q8SXZ0_DROME	RE47719p	24	56 222	1
tr Q8SY92 Q8SY92_DROME	RH21971p antennal dehydrogenase	327	27 362	5
tr Q8T3H5 Q8T3H5_DROME	AT28279p, CG13382	33	59 050	1
tr Q8T3Y1 Q8T3Y1_DROME	AT26187p, CG17440	25	42 763	1
tr Q8T487 Q8T487_DROME	AT10439p, CG1950	29	39 778	2
tr Q8T8Q5 Q8T8Q5_DROME	SD05887p, CG3493	26	170 613	2
tr Q8T9I2 Q8T9I2_DROME	GM13608p, Bip1	27	46 380	1
tr Q95RB2 Q95RB2_DROME	CG8505-PA, Cpr49Ae	94	14 501	1
tr Q95RB2 Q95RB2_DROME	CG8505-PA, Cpr49Ae	88	14 501	1
tr Q961M4 Q961M4_DROME	GH15731p	28	94 143	1
tr Q9NHV6 Q9NHV6_DROME	Dorsal interacting protein 2	37	26 140	1
tr Q9U1K3 Q9U1K3_DROME	Globin1	40	17 149	1

Table 2 Continued

Accession numbers	Protein identification	Protein score	Protein mass	Protein matches
tr Q9U3Y5 Q9U3Y5_DROME	Dynein heavy chain	25	529 605	1
tr Q9V3H9 Q9V3H9_DROME	BcDNA.LD27873	26	113 870	2
tr Q9VCW7 Q9VCW7_DROME	CG6954-PA, CG6954	29	181 921	1
tr Q9VEB1 Q9VEB1_DROME	CG7998-PA (IP09655p)	122	35 524	2
tr Q9VF51 Q9VF51_DROME	FI04488p	89	139 567	3
tr Q9VGD4 Q9VGD4_DROME	CG14741-PA	23	193 892	1
tr Q9VH97 Q9VH97_DROME	CG9492-PA	33	539 599	1
tr Q9VIK1 Q9VIK1_DROME	CG9318-PA (LD44273p)	24	75 732	2
tr Q9VQF7 Q9VQF7_DROME	CG9894-PA, isoform A (CG9894-PB, isoform B) (RE38782p)	180	15 508	3
tr Q9VQT8 Q9VQT8_DROME	CG16712-PA (RH38008p) (RH05411p)	75	9144	1
tr Q9VSY1 Q9VSY1_DROME	CG4022-PA	29	57 600	1
tr Q9VTC3 Q9VTC3_DROME	CG6409-PA (GH07049p)	86	40 356	4
tr Q9W1A9 Q9W1A9_DROME	CG11290-PA	27	257 089	2
tr Q9W246 Q9W246_DROME	CG4554-PA	27	313 818	1
tr Q9W306 Q9W306_DROME	CG9691-PA, isoform A (CG9691-PB, isoform B) (RH12290p)	57	13 081	1
tr Q9W321 Q9W321_DROME	CG15319-PB	37	343 477	2
tr Q9W3B3 Q9W3B3_DROME	CG1885-PA (GH17465p)	35	31 218	2
tr Q9W4C3 Q9W4C3_DROME	Ubiquitin carboxyl-terminal hydrolase, CG4165	38	122 838	3

the identification of 92 proteins (Table 2) with high statistical confidence. Examination of the identities of these proteins indicates that they originate both from the extracellular perilymph and from the cytoplasm of disrupted cells. We classified these proteins into 8 major categories (Table 3; Figure 2). These include enzymes involved with intermediary metabolism, primarily the glycolytic pathway, tricarboxylic acid cycle, and oxidative phosphorylation; proteins associated with regulation of gene expression, nucleic acid metabolism and protein metabolism, including regulation of transcription, histone modification and mRNA splicing, protein folding, and degradation; proteins associated with microtubular transport; Obps; protective enzymes associated with antibacterial defense and defense against oxidative damage; cuticular proteins; miscellaneous proteins associated with programmed cell death (Pcs), neuropeptide hormone activity (Nplp2), regulation of mating and courtship behavior (Esterase-6), oxygen transport (glob1), tyrosine kinase activity (Fps85D), and cell adhesion (hig); and proteins of unknown function, which represented the largest group comprising about one-third of all soluble proteins identified (Table 3; Figure 2).

We detected substantially fewer proteins in male antennal extracts than in antennal extracts from females (see Supplementary Tables 1–4). This is most likely due to greater resis-

tance to cell disruption under the conditions used in antennae from males than females, for unknown reasons. However, 6 of 8 Obps and 4 of 8 proteins associated with biotic and abiotic defense were found both in male and female antennae, suggesting that extracellular proteins in the perilymph are released effectively from male antennae and that detection of Obp44a and Obp56e in female but not male samples may reflect true sexual dimorphism in the expression of Obps, in-line with previous observations (Anholt et al. 2003). Pbprp2 (aka Obp19d), Pbprp3 (aka Os-F, Obp83a), Pbprp5 (aka Obp28a), and Pbprp6 (aka Os-E, Obp83b) have been localized previously to antennae (Pikielny et al. 1994; Hekmat-Scafe et al. 1997; Shandbag et al. 2001). In these initial experiments, we identified only 8 members of the Obp family, which comprises more than 50 Obp genes (Hekmat-Scafe et al. 2002). Notably, absent was the Lush protein (Kim et al. 1998), which mediates recognition of the male courtship pheromone 11-*cis*-vaccenylacetate in T1 trichoid sensilla of the antenna (Xu et al. 2005; Laughlin et al. 2008). It is possible that the amounts of Lush are below our detection limit. The same may be true for other members of the Obp family. Indeed, when the amount of tissue was increased from 120 to 500 antennae, we were able to detect a larger number of proteins with 10 additional Obps, including Lush, A5, Pbprp1 (aka Obp69a), Pbprp4 (aka Obp84a),

Table 3 The soluble proteome of *Drosophila melanogaster* antennae^a**Intermediary metabolism (17.4%)**

Glyceraldehyde phosphate dehydrogenase
Glycerol kinase

Aldolase

Enolase
L-Malate dehydrogenase
Citrate synthase
Isocitrate dehydrogenase
ATP synthase uncoupling factor 2
Vha44
Vha 55

Blw, ATP synthase

ATP synthase subunit B

CG6054
CG14741
CG1885
Calmodulin

Regulation of gene expression, nucleic acid metabolism, and protein metabolism (17.3%)

Taf1
Lds
Pep
Histone-lysine *N*-methyltransferase
Su(z)12
Cg11290
Vir
Nej
CG2207
CG33715

Hsp60

Ribosomal protein S3A
CG4494
CG2097
CG1950 (ubiquitin thiolesterase)
CG4165 (ubiquitin thiolesterase)

Cytoskeletal organization/microtubule movement (5.5%)**Capu**

CG4532
Klp61F

CG9492

Dynein heavy chain Kl-5

Obps (8.7%)**Pbprp2**

Pbprp3

Pbprp5

Pbprp6**A10**

Obp44a
Obp56d
Obp56e

Oxidative enzymes and defense mechanisms (8.7%)

Peroxiredoxin 1
Superoxide dismutase
GstD1
Tx1
CG6214
Glutathione peroxidase
CG13551

Table 3 Continued

Dnr1

Unknown function (33.7%)

CG17994
CG1625
CG8424
CG41561
CG8486
CG14667
Bnb (gliogenesis)
PebIII
CG14810
CG33552
CG7137
CG14141
Antdh
CG13382
CG17440
CG15296
CG3493
GH15731p
BcDNA-LD27873
CG6954
Dip2
CG9318
CG9894
CG16712
CG6409
CG4554
CG9691
CG15140
Smid
Bip1
CG4022

Structural proteins of the cuticle (2.2%)

Acp65Aa
Cpr49Ae

Miscellaneous (6.5%)

Pcs (programmed cell death)
Nplp2 (neuropeptide hormone activity)
Esterase-6 (regulation of receptivity, sperm competition, mating, pheromone synthesis, courtship behavior)
Globin 1 (oxygen transport)
Pfs85D (protein tyrosine kinase activity; photoreceptor cell morphogenesis)
Hig (cell adhesion)

^aInformation in this table is derived from Tables 2 and 3. Underlined entries designate identification in female antennae only; italic font indicates identification in male antennal extracts only; and bold font indicates identification in both male and female antennal extracts.

Obp19a, Obp47b, Obp56a, Obp59a, Obp99b, and Obp99c. Furthermore, some Obps may not be expressed in antennae. For example, some Obps are expressed in the tarsi (Galindo and Smith 2001; Matsuo et al. 2007), fat body (Fujii and Amrein 2002), or male accessory gland (Takemori and Yamamoto 2009) and therefore would not be detected in the antenna.

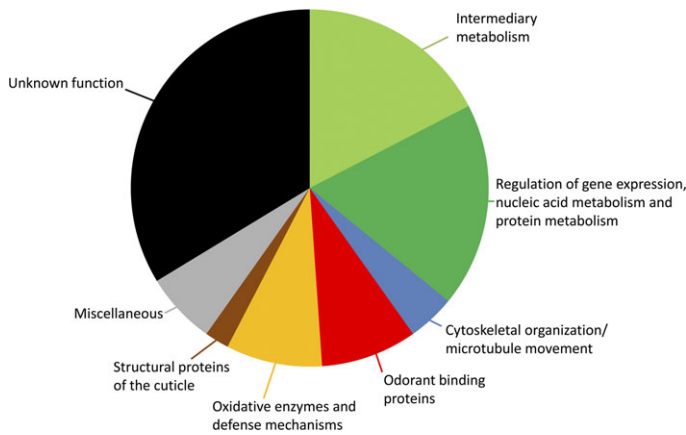


Figure 2 The number of soluble proteins in different functional categories detected in *Drosophila* antennae. See also Table 3.

The vast majority of proteins we detected are widely expressed in many or all cells. Nevertheless, their functions in different cells are essential for enabling distinct physiological functions. For example, intermediary metabolism is necessary to provide energy for olfactory signal transduction, and cytoskeletal organization is essential for maintaining dendritic and axonal structure and function. Two of the categories of soluble proteins indicated in Table 3 are specifically relevant to chemosensation: Obps, which are essential for the transport of hydrophobic odorants in the perilymph, and oxidative enzymes and defense mechanisms which likely contribute to cytochrome P450-mediated inactivation or degradation of odorants and environmental toxins. Obps have been defined based on their structure, including the characteristic positions of disulfide bonds (Hekmat-Scafe et al. 2002). However, olfactory functions have been ascribed to only few members of this family and other possible functions, such as a carrier function for molecules transmitted between males and females during mating have also been noted. Altered regulation of expression of *Obp* genes has been observed following mating (McGraw et al. 2004; Zhou et al. 2009) and after exposure to starvation stress (Harbison et al. 2005) or alcohol intoxication (Morozova et al. 2006). In addition, changes in expression levels of *Obp* genes occur as a correlated response to artificial selection for divergent levels of copulation latency (Mackay et al. 2005) and aggression (Edwards et al. 2006), and expression levels change during social crowding and as a result of ageing (Zhou et al. 2009). Systems genetics analyses of 6 X chromosome linked *Obp* genes showed that their transcripts form part of diverse transcriptional network niches, associated with olfactory behavior, synaptic transmission, detection of signals regulating tissue development and apoptosis, postmating behavior and oviposition, and nutrient sensing (Arya GH, Weber AL, Wang P, Magwire MM, Serrano Negron YL, Mackay TFC, Anholt RRH, unpublished data). Our proteomics analysis has identified Obps that are expressed in the antenna

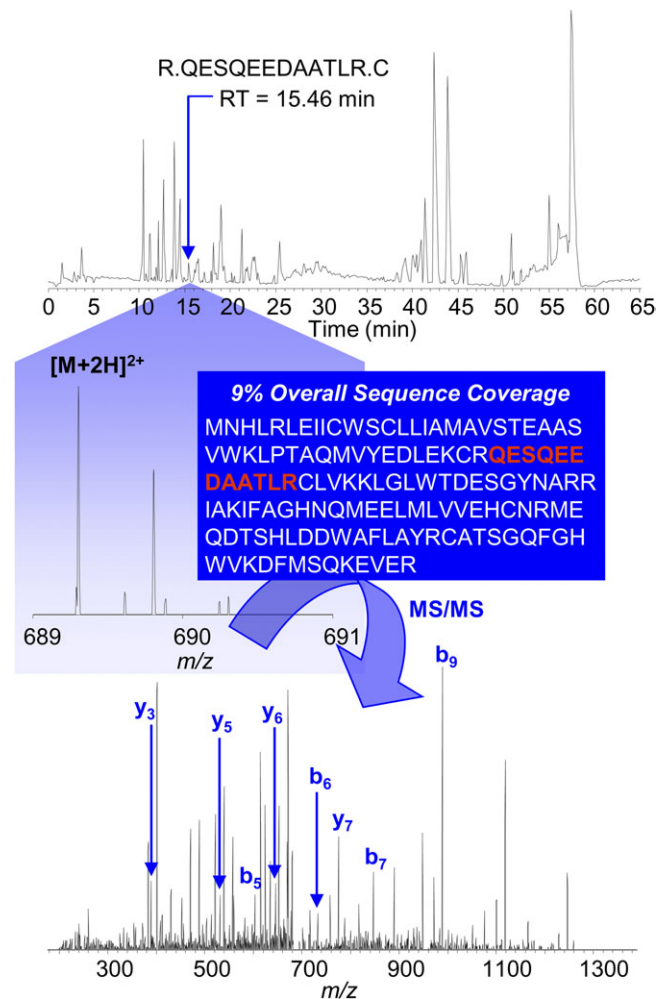


Figure 3 nano-LC/MS/MS identification of tr[Q9VAI7]Q9VAI7_DROME CG15505-PA (Obp 99d). A tryptic peptide, which eluted from the nano-LC column at a retention time (RT) of 15.46 min (chromatogram shown at the top of the figure), is identified by nano-LC/MS/MS (with database searching) to be derived from Obp99d. The MS spectrum for this peptide is shown in the center of the figure. The ionized, doubly charged peptide is subjected to dynamic exclusion and fragmentation to generate an MS/MS fingerprint (lower spectrum) that conclusively verifies its molecular structure. In contrast to PBPRP2 (Figure 1), which is present in abundance and identified by 11 tryptic peptides (Tables 1 and 2), a single peptide (indicated in red font in the middle of the figure) was detected from the Obp99d protein and accounts for only 9% of its sequence but is sufficient to identify this low abundance Obp in the antennal extract.

and thus are candidates for contributing directly to chemosensation.

Although the second antennal segment might also contribute to the proteomics profile, the fact that Obps make up a substantial fraction of the soluble proteome (Figure 2) suggests that the major contribution to the mass spectrometric profile is derived from the third antennal segment.

An additional caveat is the notion that protein detection could be limited by masking of peptide fragments in the nano-LC/MS/MS analyses. Comigration on the LC might

also have prevented the detection of Lush or other Obps. This problem is likely to be more severe with increasing complexity of the chromatogram and more likely to impact proteins that yield few tryptic fragments, as well as those present in very low concentrations, relative to others. In addition, variations in ionization efficiencies of different peptides can lead to diminished representation in the nano-LC/MS/MS run. Furthermore, it should be noted that the proteins presented in Tables 1 and 2 represent only those that attain a high confidence score with Sequest and Mascot, respectively. Increasing the number of antennae in each sample greatly increases the number of proteins that can be interrogated by nano-LC/MS/MS approaches. This improves the chances for unambiguous identification of proteins such as *Obp99d* (Figure 3),—previously implicated in responses to benzaldehyde (Wang et al. 2007)—which, while detected by Sequest, did not produce a very confident identification and therefore is not included in Table 1, and Mascot did not allow for the identification of this protein. Nevertheless, information about the presence of *Obp99d*, which is present in low abundance, can still be extracted from the chromatogram (Figure 3).

Finally, whereas integration of chromatographic peaks can establish relative amounts of proteins represented in the sample, precise quantitative determination requires stable isotope labeled internal standard peptides. This approach is now feasible for targeted determination of specific soluble proteins of the antenna.

Supplementary material

Supplementary material can be found at <http://www.chemse.oxfordjournals.org/>

Funding

National Institutes of Health grant [GM059469].

Acknowledgements

We thank Steven A. West for excellent technical assistance and Professor David C. Muddiman (Department of Chemistry, North Carolina State University) for use of the LTQ-FT-MS in his laboratory.

References

- Andrews GL, Shuford CM, Burnett JC Jr, Hawkridge AM, Muddiman DC. 2009. Coupling of a vented column with splitless nanoRPLC-ESI-MS for the improved separation and detection of brain natriuretic peptide-32 and its proteolytic peptides. *J Chromatogr B Analyt Technol Biomed Life Sci.* 877:948–954.
- Anholt RRH, Dilda CL, Chang S, Fanara JJ, Kulkarni NH, Ganguly I, Rollmann SM, Kamdar KP, Mackay TFC. 2003. The genetic architecture of odor-guided behavior in *Drosophila*: epistasis and the transcriptome. *Nat Genet.* 35:180–184.
- Anholt RRH, Lyman RF, Mackay TFC. 1996. Effects of single P-element insertions on olfactory behavior in *Drosophila melanogaster*. *Genetics.* 143:293–301.
- Benton R, Sachse S, Michnick SW, Vosshall LB. 2006. Atypical membrane topology and heteromeric function of *Drosophila* odorant receptors in vivo. *PLoS Biol.* 4:e20.
- Benton R, Vannice KS, Gomez-Diaz C, Vosshall LB. 2009. Variant ionotropic glutamate receptors as chemosensory receptors in *Drosophila*. *Cell.* 136:149–162.
- de Bruyne M, Clyne PJ, Carlson JR. 1999. Odor coding in a model olfactory organ: the *Drosophila* maxillary palp. *J Neurosci.* 19:4520–4532.
- de Bruyne M, Foster K, Carlson JR. 2001. Odor coding in the *Drosophila* antenna. *Neuron.* 30:537–552.
- Clyne PJ, Warr CG, Freeman MR, Lessing D, Kim J, Carlson JR. 1999. A novel family of divergent seven-transmembrane proteins: candidate odorant receptors in *Drosophila*. *Neuron.* 22:327–338.
- Edwards AC, Rollmann SM, Morgan TJ, Mackay TFC. 2006. Quantitative genomics of aggressive behavior in *Drosophila melanogaster*. *PLoS Genet.* 2:e154.
- Eng JK, McCormack AL, Yates JR III. 1994. An approach to correlate tandem mass spectral data of peptides with amino acid sequences in a protein database. *J Am Soc Mass Spectrom.* 5:976–989.
- Fujii S, Amrein H. 2002. Genes expressed in the *Drosophila* head reveal a role for fat cells in sex-specific physiology. *EMBO J.* 21:5353–5363.
- Galindo K, Smith DP. 2001. A large family of divergent *Drosophila* odorant-binding proteins expressed in gustatory and olfactory sensilla. *Genetics.* 159:1059–1072.
- Gao Q, Chess A. 1999. Identification of candidate *Drosophila* olfactory receptors from genomic DNA sequence. *Genomics.* 60:31–39.
- Hallem EA, Carlson JR. 2006. Coding of odors by a receptor repertoire. *Cell.* 125:143–160.
- Hallem EA, Ho MG, Carlson JR. 2004. The molecular basis of odor coding in the *Drosophila* antenna. *Cell.* 117:965–979.
- Harbison ST, Chang S, Kamdar KP, Mackay TFC. 2005. Quantitative genomics of starvation stress resistance in *Drosophila*. *Genome Biol.* 6:R36.
- Hekmat-Scafe DS, Scafe CR, McKinney AJ, Tanouye MA. 2002. Genome-wide analysis of the odorant-binding protein gene family in *Drosophila melanogaster*. *Genome Res.* 12:1357–1369.
- Hekmat-Scafe DS, Steinbrecht RA, Carlson JR. 1997. Coexpression of two odorant-binding protein homologs in *Drosophila*: implications for olfactory coding. *J Neurosci.* 17:1616–1624.
- Kim MS, Repp A, Smith DP. 1998. LUSH odorant-binding protein mediates chemosensory responses to alcohols in *Drosophila melanogaster*. *Genetics.* 150:711–721.
- Laughlin JD, Ha TS, Jones DN, Smith DP. 2008. Activation of pheromone-sensitive neurons is mediated by conformational activation of pheromone-binding protein. *Cell.* 133:1255–1265.
- Mackay TFC, Heinsohn SL, Lyman RF, Moehring AJ, Morgan TJ, Rollmann SM. 2005. Genetics and genomics of *Drosophila* mating behavior. *Proc Natl Acad Sci USA.* 102:6622–6629.
- Matsuo T, Sugaya S, Yasukawa J, Aigaki T, Fuyama Y. 2007. Odorant-binding proteins OBP57d and OBP57e affect taste perception and host-plant preference in *Drosophila sechellia*. *PLoS Biol.* 5:e118.
- McGraw LA, Gibson G, Clark AG, Wolfner MF. 2004. Genes regulated by mating, sperm, or seminal proteins in mated female *Drosophila melanogaster*. *Curr Biol.* 14:1509–1514.

- McKenna MP, Hekmat-Scafe DS, Gaines P, Carlson JR. 1994. Putative *Drosophila* pheromone-binding proteins expressed in a subregion of the olfactory system. *J Biol Chem.* 269:16340–16347.
- Morozova TV, Anholt RRH, Mackay TFC. 2006. Transcriptional response to alcohol exposure in *Drosophila melanogaster*. *Genome Biol.* 7:R95.
- Perkins DN, Pappin DJC, Creasy DM, Cottrell JS. 1999. Probability-based protein identification by searching sequence databases using mass spectrometry data. *Electrophoresis.* 20:3551–3567.
- Pikielny CW, Hasan G, Rouyer F, Rosbash M. 1994. Members of a family of *Drosophila* putative odorant-binding proteins are expressed in different subsets of olfactory hairs. *Neuron.* 12:35–49.
- Riesgo-Escovar J, Woodard C, Gaines P, Carlson J. 1992. Development and organization of the *Drosophila* olfactory system: an analysis using enhancer traps. *J Neurobiol.* 23:947–964.
- Rollmann SM, Mackay TFC, Anholt RRH. 2005. Pinocchio, a novel protein expressed in the antenna, contributes to olfactory behavior in *Drosophila melanogaster*. *J Neurobiol.* 63:146–158.
- Sato K, Pellegrino M, Nakagawa T, Nakagawa T, Vosshall LB, Touhara K. 2008. Insect olfactory receptors are heteromeric ligand-gated ion channels. *Nature.* 452:1002–1006.
- Shanbhag SR, Hekmat-Scafe D, Kim MS, Park SK, Carlson JR, Pikielny C, Smith DP, Steinbrecht RA. 2001. Expression mosaic of odorant-binding proteins in *Drosophila* olfactory organs. *Microsc Res Tech.* 55:297–306.
- Takemori N, Yamamoto MT. 2009. Proteome mapping of the *Drosophila melanogaster* male reproductive system. *Proteomics.* 9:2484–2493.
- Vosshall LB, Amrein H, Morozov PS, Rzhetsky A, Axel R. 1999. A spatial map of olfactory receptor expression in the *Drosophila* antenna. *Cell.* 96:725–736.
- Vosshall LB, Wong AM, Axel R. 2000. An olfactory sensory map in the fly brain. *Cell.* 102:147–159.
- Wang P, Lyman RF, Shabalina SA, Mackay TFC, Anholt RRH. 2007. Association of polymorphisms in odorant-binding protein genes with variation in olfactory response to benzaldehyde in *Drosophila*. *Genetics.* 177:1655–1665.
- Wicher D, Schäfer R, Bauernfeind R, Stensmyr MC, Heller R, Heinemann SH, Hansson BS. 2008. *Drosophila* odorant receptors are both ligand-gated and cyclic-nucleotide-activated cation channels. *Nature.* 452:1007–1011.
- Xu P, Atkinson R, Jones DN, Smith DP. 2005. *Drosophila* OBP LUSH is required for activity of pheromone-sensitive neurons. *Neuron.* 45:193–200.
- Zhou S, Atkinson EA, Mackay TFC, Anholt RRH. Forthcoming 2009. Plasticity of the chemoreceptor repertoire in *Drosophila melanogaster*. *PLoS Genet.* 5:e1000681.